Supplementary Information

Synthesis of $CoSe_2$ reinforced nitrogen-doped carbon composites as advanced anode for potassium-ion batteries

Guowei Yang,[a,1] Chengzhan Yan,[b,1] Ping Hu,[a] Qun Fu,[a] Huaping Zhao,[b] and Yong Lei[b,*]

[a]Institute of Nanochemistry and Nanobiology, School of Environmental and Chemical Engineering, Shanghai University, Shanghai 200444, China

[b]Fachgebiet Angewandte Nanophysik, Institut für Physik & ZMN MacroNano (ZIK), Technische Universität Ilmenau, Ilmenau 98693, Germany

[1]Guowei Yang and Chengzhan Yan contributed equally to this work.

Corresponding Author:

* E-mail: yong.lei@tu-ilmenau.de

Experimental section

Materials synthesis

Synthesis of $CoSe_2$ nanosheets: $CoSe_2$ nanosheets were prepared through a facile hydrothermal method. In details, cobalt acetate tetrahydrate (0.498 g), selenium (0.3158 g), and citric acid (4 g) were dispersed in deionized water (44 mL), then hydrazine hydrate (16 mL) was added. The mixture was magnetically stirred for 30 minutes, and then was transferred into a 100 mL Teflon-lined stainless-steel autoclave. The autoclave was kept at 150 ℃ for 16 h. After cooling down to room temperature, the formed gray powder was collected and washed with deionized water and absolute ethanol, and then

dried under vacuum at 60 °C overnight.

Synthesis of $CoSe_2$@C composites: $CoSe_2$ nanosheets (300 mg) was dispersed in Tris (tris(hydroxymethyl) aminomethane) buffer solution (150 mL) under ultrasonication and stirred for 30 min. Then, dopamine hydrochloride (300 mg) was dispersed in this mixed solution, and the mixture was continuously stirred at room temperature for 48 h to obtain $CoSe_2$@PDA. The formed black powder was collected and washed with deionized water and absolute ethanol, and then dried under vacuum at 60 °C overnight. Finally, $CoSe_2$@PDA was calcined at 500 °C with a heating rate of 3 °C/min under an Ar atmosphere for 3 h. The obtained product was named as $CoSe_2$@C-1:1. For comparison, similar procedure was followed to synthesize $CoSe_2$ (300 mg: 0 mg), $CoSe_2$@C-1:0.25 (300 mg: 75 mg), $CoSe_2$@C-1:0.5 (300 mg: 150 mg), $CoSe_2$@C-1:2 (300 mg: 600 mg), and pure carbon (0 mg: 300 mg) by only changing the mass ratio of $CoSe_2$ nanosheets and dopamine hydrochloride.

Material characterizations

The compositions of the samples were characterized with X-ray diffraction (Smartlab X-ray Diffractometer), X-ray photoelectron spectroscopy (Thermo Scientific K-Alpha), and Raman spectroscopy (inVia Qontor/Renishaw inVia Qontor) with a laser wavelength of 514 nm. Scanning electron microscopy (SEM) analysis was conducted using a field-emission scanning electron microscope (JEOL JSM-7500F). Transmission electron microscopy (TEM) analysis was performed on transmission electron microscope (JEOL JEM 2100F and JEOL JEM 2011Plus). The content of $CoSe_2$ was determined via the thermogravimetric analysis (TGA) instrument (TGA5500) under an

oxygen atmosphere at temperatures ranging from 30 to 800 °C at a heating rate of 20 °C/min. The specific surface areas and pore-size distributions were calculated from the nitrogen (N_2) adsorption/desorption isotherm data (recorded at 77.3 K under liquid nitrogen) using Micromeritics ASAP 2420.

Electrochemical measurements.

All half-cell tests were performed in CR2032 coin cell cases. The working electrode was composed of active material, carbon black (Super P), and carboxymethyl cellulose sodium (CMC) in a weight ratio of 7:2:1, and were uniformly mixed in an aqueous solution. Then the slurry was uniformly coated on copper foils, dried overnight at 60 °C in a vacuum oven. The coated copper foils were cut into small discs with a diameter of 16 mm by a slicing device, and the active material loading on it was about 1 mg. The electrolytes were chosen to use 2.0 M potassium bis(fluorosulfonyl)imide (KFSI) dissolved in ethylene carbonate (EC) and diethylene carbonate (DEC) (V_{EC}/V_{DEC}=1:1). The separator was Whatman glass fibers, and the counter electrode was potassium metal foil. The half-cells were assembled in an argon-filled glove box and tested using a Land CT 2001A battery system (Land, China) with a voltage range of 0.01–3 V. Cyclic voltammetry (CV) and electrochemical impedance spectroscopy (EIS) were performed on a VMP3 electrochemical workstation with a voltage range of 0.01-3 V.

Supporting figures

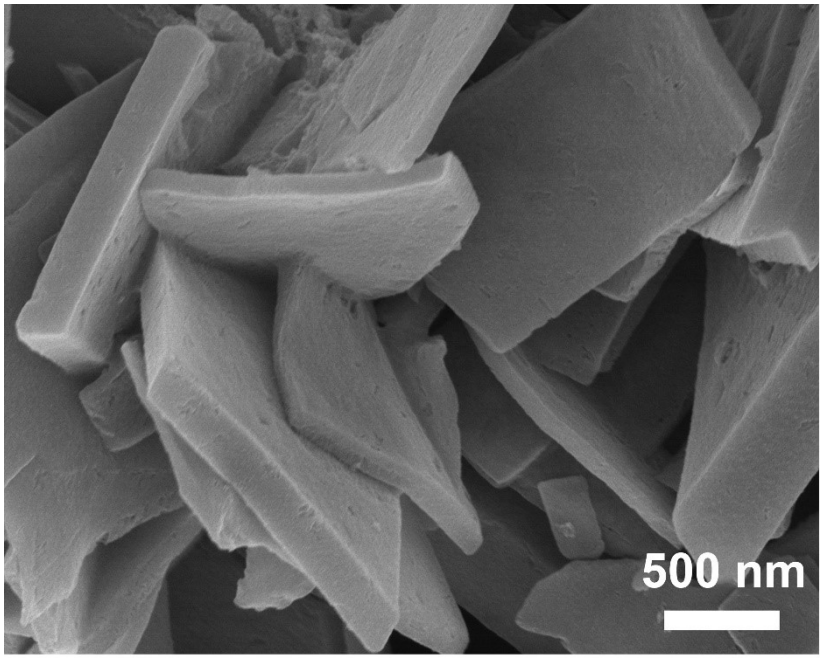

Figure S1. SEM image of $CoSe_2$ nanosheets.

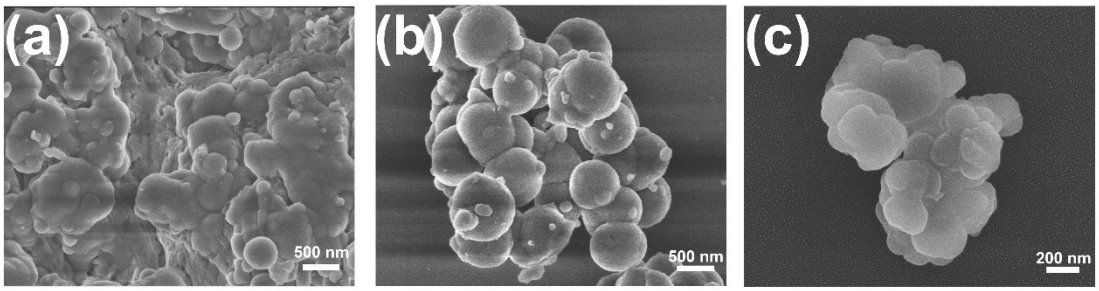

Figure S2. SEM images of (a) $CoSe_2$@PDA-1:0.25. (b) $CoSe_2$@PDA-1:0.5, and (c) $CoSe_2$@PDA-1:1.

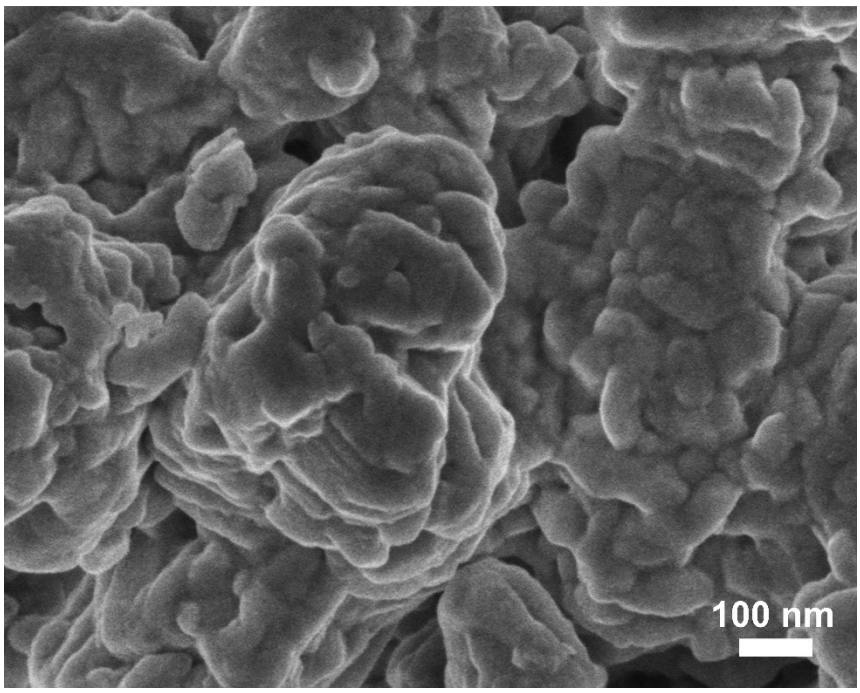

Figure S3. SEM images of $CoSe_2$ treated with hydrochloric acid and Tris buffer solution.

Experimental scheme: referring to the synthesis process of $CoSe_2$@C-1:1, 300mg of $CoSe_2$ was added to 150ml of Tris buffer solution, and 0.266ml of concentrated hydrochloric acid (concentration of 36%-38%) was added and stirred for 48h.

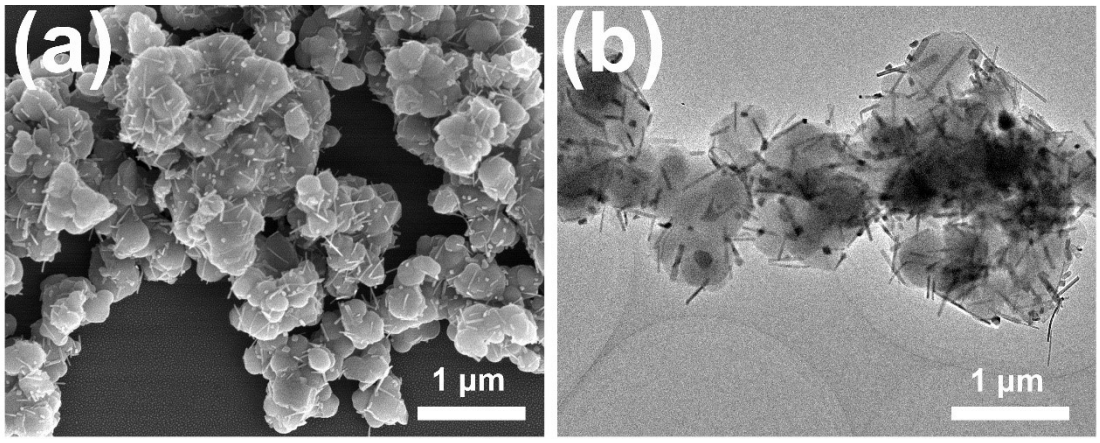

Figure S4. (a) and (b) SEM and TEM images of $CoSe_2$@C-1:2.

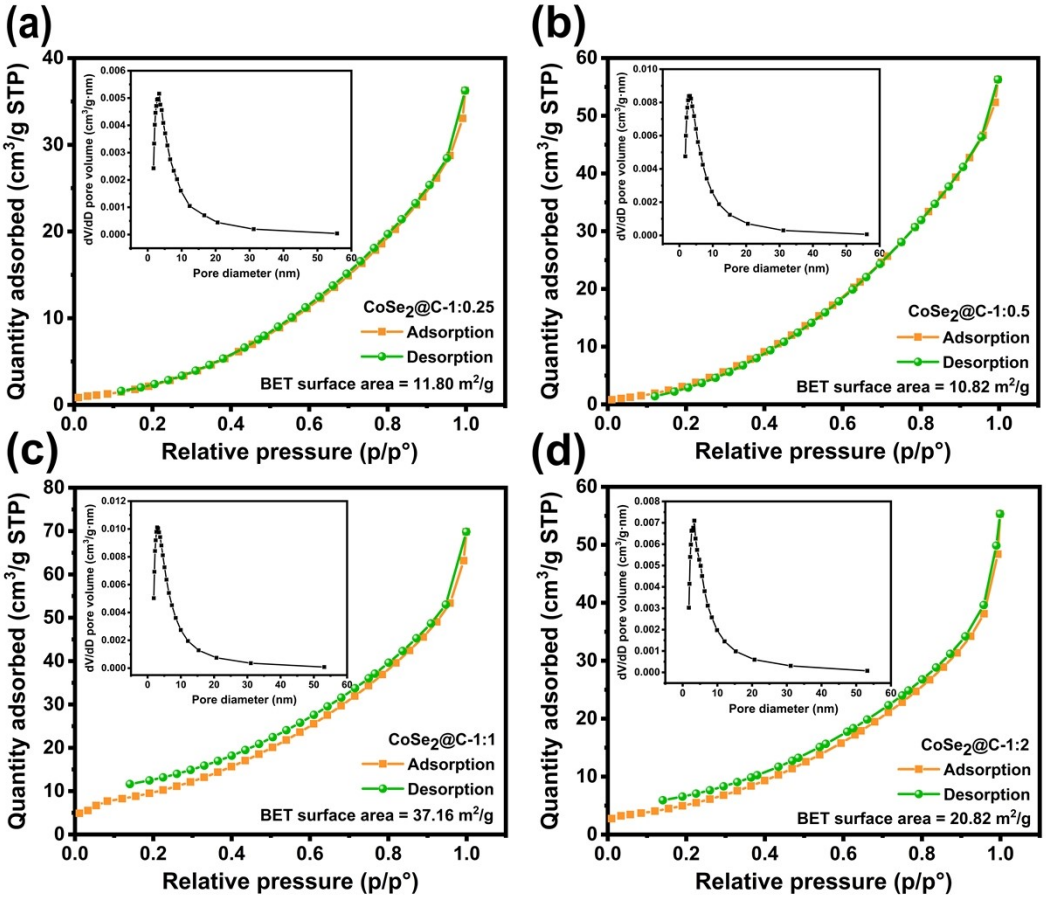

Figure S5. Nitrogen adsorption-desorption isotherms and pore size distribution (insert) of (a) $CoSe_2$@C-1:0.25, (b) $CoSe_2$@C-1:0.5, (c) $CoSe_2$@C-1:1, and (d) $CoSe_2$@C-1:2.

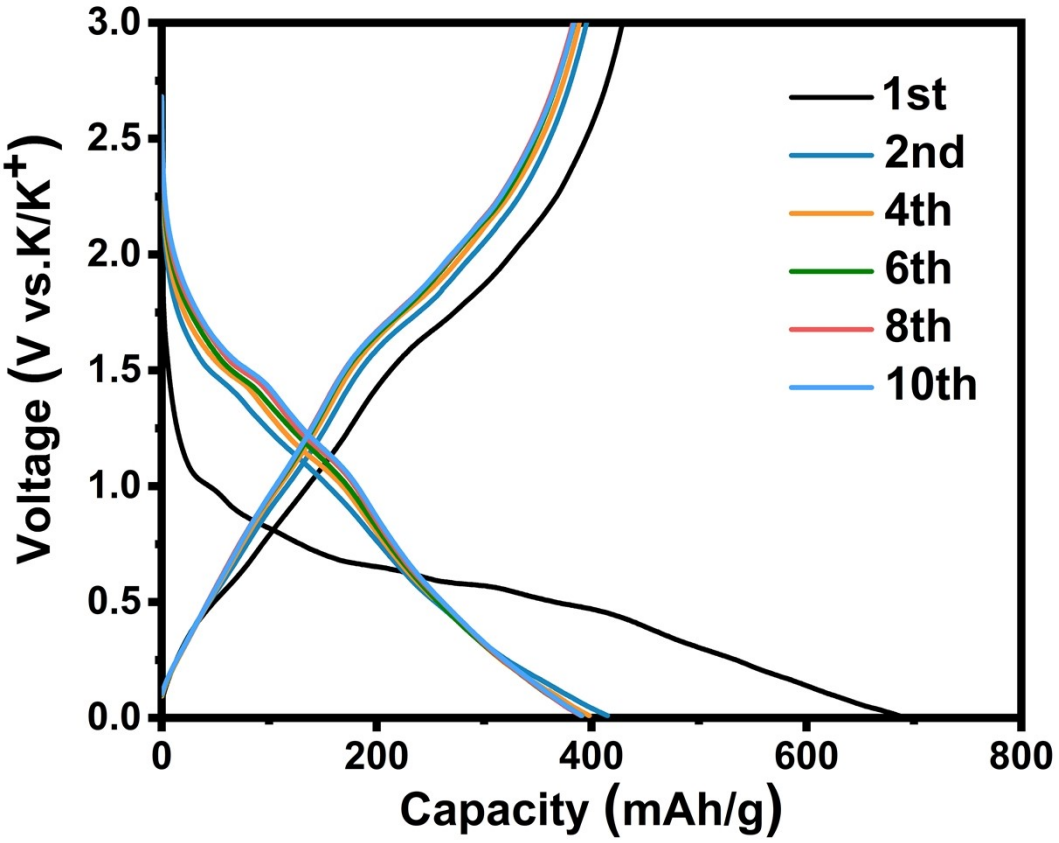

Figure S6. Discharge/charge profiles of $CoSe_2$@C-1:1 within the potential of 0.01-3 V at a current density of 0.1 A/g.

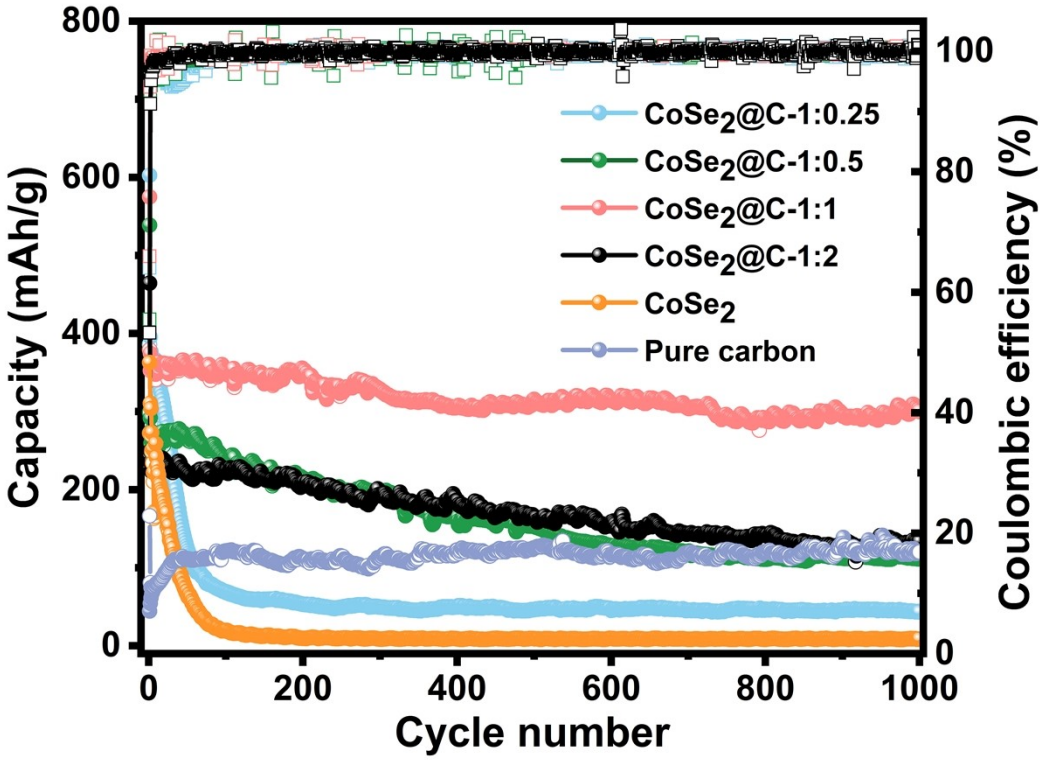

Figure S7. Cycling performance of $CoSe_2$, pure carbon, and the as-synthesized $CoSe_2$@C composites at current densities of 0.5 A/g.

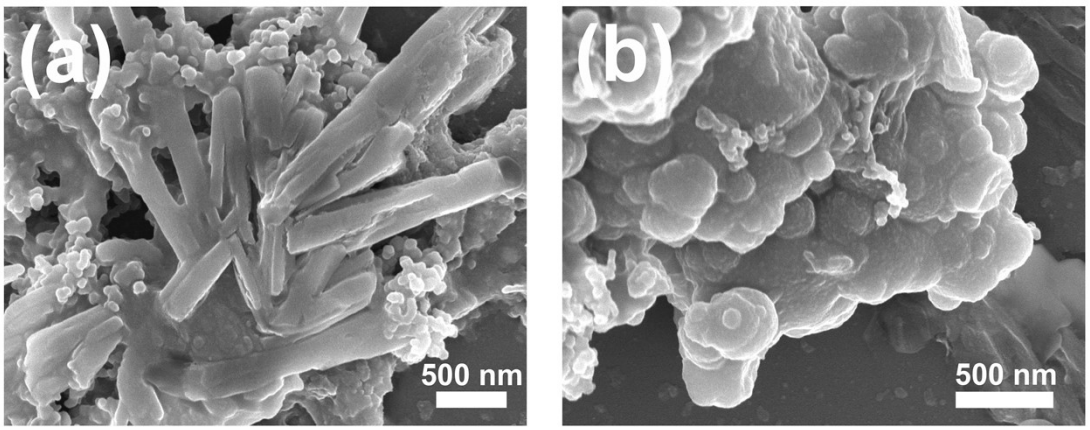

Figure S8. SEM images of (a) $CoSe_2$, and (b) $CoSe_2$@C-1:1 after 200 cycles.

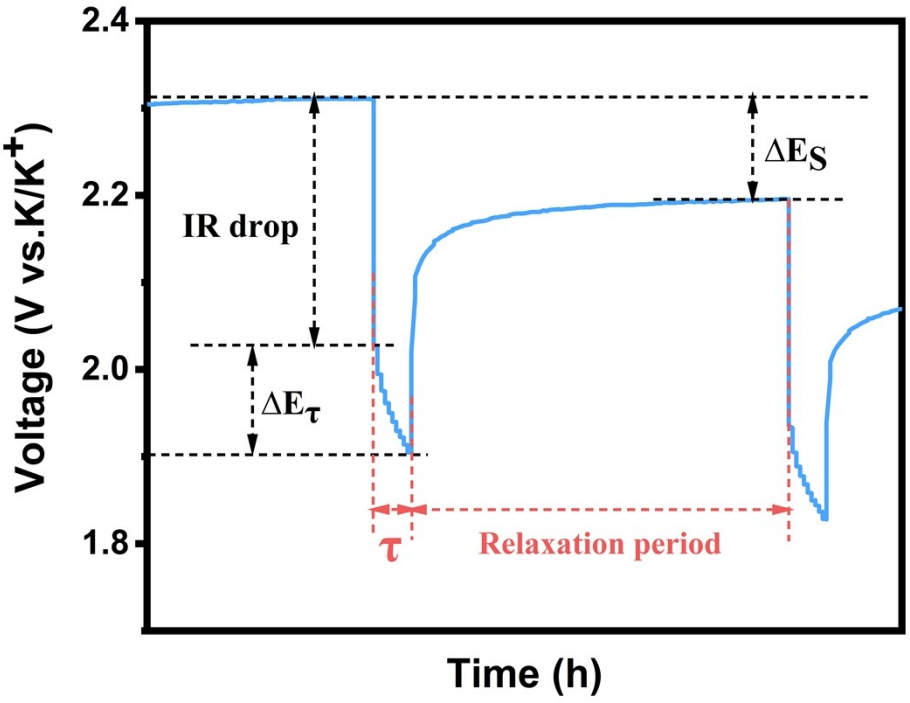

Figure S9. Schematic illustration of selected steps from the GITT profile during charging.

According to Fick's second law, the value of dk can be calculated by the following equation:

$$D_K = \frac{4}{\pi\tau}\left(\frac{m_B V_M}{M_B S}\right)^2\left(\frac{\Delta E_S}{\Delta E_\tau}\right)^2\left(t \ll \frac{L_2}{D}\right)$$

where τ is the pulse time (s), m_B is the mass of active materials, and V_M is the molar volume ($cm^3\ mol^{-1}$), M_B is the molar mass of the active materials, S is the area of the electrode, ΔE_S and ΔE_τ are defined in Figure S5.[11]

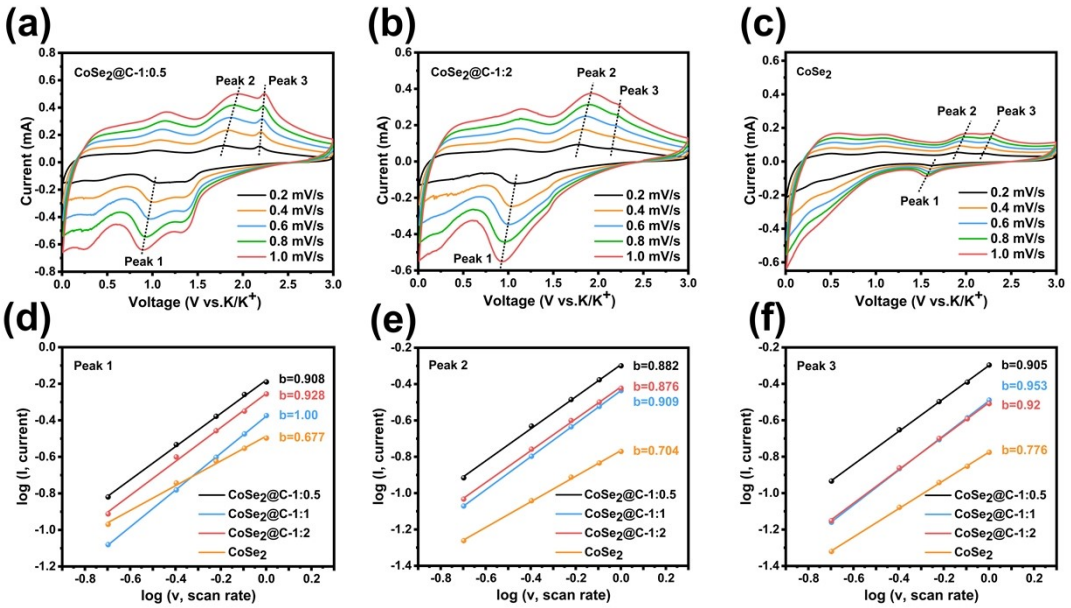

Figure S10. CV curves of (a) $CoSe_2$@C-1:0.5 (b) $CoSe_2$@C-1:2, and (c) $CoSe_2$ composite electrode at various scan rates of 0.2-1.0 mV/s. log (i) *versus* log (v) plots at (d) peak 1, (e) peak 2, and (f) peak 3.

Table S1. Comparison of some representative anodes in potassium-ion batteries.

Samples	Initial coulombic efficiency	Cyclic stability at a low current density	Rate capability		Cyclic stability at a high current density.	Ref.
			Capacity	Current densities		
$CoSe_2$@C-1:1	**62.5%**	**366.1 mAh/g after 100 cycles at 0.1 A/g**	**457.5, 447.1, 437.5, 414.5, 396.1, 366, 333.8, and 281.5 mAh/g**	**0.05, 0.1, 0.2, 0.3, 0.5, 1.0, 2.0, and 5.0 A/g**	**237.6 mAh/g after 1000 cycles at 1.0 A/g**	**This work**
N/S co-doped carbon nanocapsule	33%	309 mAh/g after 100 cycles at 0.1 A/g	408, 345, 285, 236, 201,173, and 149 mAh/g	0.05, 0.1, 0.2, 0.5, 1.0, 2.0, and 5.0 A/g	150 mAh/g after 2000 cycles at 2 A/g	1
Ni_2P@NPC	24.7%	282 mAh/g after 100 cycles at 0.1 A/g	355, 279, 242, 203, 158, and 114 mAh/g	0.1, 0.2, 0.5, 1.0, 2.0, and 5.0 A/g	212 mAh/g after 5000 cycles at 1.0 A/g	2
π-conjugated polypyrene porous nanoflowers	35.2%	302 mAh/g after 60 cycles at 0.1 A/g	From 220 to 165 mAh/g	0.05, 0.1, 0.2, 0.4, 0.8, and 1.6 A/g	190 mAh/g after 1000 cycles at 0.5 A/g	3
Sb_2MoO_6/rGO	55.7%	381 mAh/g after 50 cycles at 0.2 A/g	402, 350, 248, and 161 mAh/g	0.1, 0.2, 0.5, and 1.0 A/g	247 mAh/g after 100 cycles at 0.5 A/g	4

VS_2/N-C@rGO	61.2%	334 mAh/g after 300 cycles at 0.2 A/g	409, 391, 362, 337, 321, 299, and 273 mAh/g	0.1, 0.2, 0.5, 1.0, 2.0, 4.0, and 8.0 A/g	216 mAh/g after 500 cycles at 1.0 A/g	5
VSe_2 nanosheets	69.1%	335 mAh/g after 200 cycles at 0.2 A/g	374, 350, 334, 269 and 172 mAh/g	0.1, 0.2, 0.5, 1.0, and 2.0 A/g	~150 mAh/g after 500 cycles at 2.0 A/g	6
$FeSe_2$/PCN	72.1%	330 mAh/g after 100 cycles at 0.1 A/g	752, 790, 803, 810, 766, 672, and 523 mAh/g	0.1, 0.2, 0.5, 1.0, 2.0, 5.0, and 10.0 A/g	128 mAh/g after 500 cycles at 2.0 A/g	7
$MoSe_2$/rGO nanosheets	54.5%	310 mAh/g after 50 cycles at 0.1 A/g	279.2,220.4, 155.2, and 77.8 mAh/g	0.2, 0.5, 1.0, and 2.0 A/g	Null	8
$CoSe_2$/NC/HMCS	66%	442 mAh/g after 120 cycles at 0.1 A/g	394, 363, 324, 298, and 263 mAh/g	0.1, 0.2, 0.5, 1.0, and 2.0 A/g	Null	9
$CoSe_2$ nanosheets on 3D N-doped carbon foam (CSNS/NCF)	70%	335 mAh/g after 200 cycles at 0.05 A/g	352, 334, 298, 270, 243, and 226 mAh/g	0.05, 0.1, 0.2, 0.5, 1.0, and 2.0 A/g	198 mAh/g after 1000 cycles at 1.0 A/g	10

Table S2. The R_{ct} values of each electrode material after 1 cycle and 100 cycles.

Sample	R_{ct} (Ω)	
	1st	100th
$CoSe_2$@C-1:0.5	260.5	1115
$CoSe_2$@C-1:1	102.1	540.7
$CoSe_2$@C-1:2	335.6	1066

Reference

1. H. Bi, X. He, L. Yang, H. Li, B. Jin and J. Qiu, Interconnected carbon nanocapsules with high N/S co-doping as stable and high-capacity potassium-ion battery anode, *J. Energy Chem.*, 2022, **66**, 195-204.
2. Z. Yan, Z. Huang, Y. Yao, X. Yang, H. Li, C. Xu, Y. Kuang and H. Zhou, Monodispersed Ni_2P nanodots embedded in N, P co-doped porous carbon as super stable anode material for potassium-ion batteries, *J. Alloy. Compd.*, 2021,

858, 158203.

3. H. Li, J. Wu, H. Li, Y. Xu, J. Zheng, Q. Shi, H. Kang, S. Zhao, L. Zhang, R. Wang, S. Xin, T. Zhou and C. Zhang, Designing pi-conjugated polypyrene nanoflowers formed with meso- and microporous nanosheets for high-performance anode of potassium ion batteries, *Chem. Eng. J.*, 2022, **430**, 132704.

4. J. Wang, B. Wang, Z. Liu, L. Fan, Q. Zhang, H. Ding, L. Wang, H. Yang, X. Yu and B. Lu, Nature of bimetallic oxide Sb_2MoO_6/rGO anode for high-performance potassium-ion batteries, *Adv. Sci.*, 2019, **6**, 1900904.

5. J. Sun, G. Lian, L. Jing, D. Wu, D. Cui, Q. Wang, H. Yu, H. Zhang and C. P. Wong, Assembly of flower-like VS_2/N-doped porous carbon with expanded (001) plane on rGO for superior Na-ion and K-ion storage, *Nano Res.*, 2022, **15**, 4108-4116.

6. C. Yang, J. Feng, F. Lv, J. Zhou, C. Lin, K. Wang, Y. Zhang, Y. Yang, W. Wang, J. Li and S. Guo, Metallic graphene-like VSe_2 ultrathin nanosheets: superior potassium-ion storage and their working mechanism, *Adv. Mater.*, 2018, **30**, 1800036.

7. W. Zhao, Q. Tan, K. Han, D. He, P. Li, M. Qin and X. Qu, Achieving fast and stable lithium/potassium storage by in situ decorating $FeSe_2$ nanodots into three-dimensional hierarchical porous carbon networks, *J. Phys. Chem. C*, 2020, **124**, 12185-12194.

8. S. Chong, X. Wei, Y. Wu, L. Sun, C. Shu, Q. Lu, Y. Hu, G. Cao and W. Huang,

Expanded $MoSe_2$ nanosheets vertically bonded on reduced graphene oxide for sodium and potassium-ion storage, *ACS Appl. Mater. Interfaces*, 2021, **13**, 13158-13169.

9. S. H. Yang, S.-K. Park and Y. C. Kang, MOF-derived $CoSe_2$@N-doped carbon matrix confined in hollow mesoporous carbon nanospheres as high-performance anodes for potassium-ion batteries, *Nano-Micro Lett.*, 2021, **13**, 9.

10. G. Suo, J. Zhang, D. Li, Q. Yu, W. Wan, M. He, L. Feng, X. Hou, Y. Yang, X. Ye and L. Zhang, N-doped carbon/ultrathin 2D metallic cobalt selenide core/sheath flexible framework bridged by chemical bonds for high-performance potassium storage, *Chem. Eng. J.*, 2020, **388**, 124396.

11. X. Zhao, C. Zhang, G. Yang, Y. Wu, Q. Fu, H. Zhao and Y. Lei, Bismuth selenide nanosheets confined in thin carbon layers as anode materials for advanced potassium-ion batteries, *Inorg. Chem. Front.*, 2021, **8**, 4267.